

Interface effect in QCD phase transitions via Dyson-Schwinger equation approach

Fei Gao^{1,2} and Yu-xin Liu^{1,2,3,*}

¹*Department of Physics and State Key Laboratory of Nuclear Physics and Technology, Peking University, Beijing 100871, China*

²*Collaborative Innovation Center of Quantum Matter, Beijing 100871, China*

³*Center for High Energy Physics, Peking University, Beijing 100871, China*

(Received 28 September 2016; published 23 November 2016)

With the chiral susceptibility criterion, we obtain the phase diagram of strong-interaction matter in terms of temperature and chemical potential in the framework of Dyson-Schwinger equations of QCD. After calculating the pressure and some other thermodynamic properties of the matter in the Dyson-Schwinger method, we get the phase diagram in terms of temperature and baryon number density. We also obtain the interface tension and the interface entropy density to describe the inhomogeneity of the two phases in the coexistence region of the first-order phase transition. After including the interface effect, we find that the total entropy density of the system increases in both the deconfinement (dynamical chiral symmetry restoration) and the hadronization (dynamical chiral symmetry breaking) processes of the first-order phase transitions and thus solve the entropy puzzle in the hadronization process.

DOI: 10.1103/PhysRevD.94.094030

I. INTRODUCTION

The phase transitions of strong-interaction matter (QCD phase transitions) with respect to temperature T and chemical potential μ have been investigated for a long time (see, e.g., Refs. [1–6]). On the theoretical side, the studies include effective model calculations (see, e.g., Refs. [1,7–22]), the Dyson-Schwinger equation method (see, e.g., Refs. [23–42]), functional renormalization group approach (see, e.g., Refs. [43–48]), and lattice QCD simulations (see, e.g., Refs. [49–73]). Based on these, it has been widely accepted that at physical quark mass the chiral phase transition is a crossover at low chemical potential, while it is a first-order phase transition at high chemical potential. Meanwhile, the confinement-deconfinement phase transition coincides with the chiral phase transition (see, e.g., Refs. [22,37,41,42]).

The first-order phase transition is generally described by process of either nucleation or explosive spinodal decomposition [74]. With the chiral susceptibility criteria (see, e.g., Refs. [17,20,28,30,75]), one usually finds the phase transition as a nucleation process which is defined as the transition from a metastable phase to a stable phase, and the stable phase boundary and the metastable phase boundary determine the coexistence region. Astrophysical observables of compact stars also favor the nucleation of quark matter [74,76–80]. When the first-order phase transition takes place, the two phases with different thermal properties, the dynamical chiral symmetry breaking (DCSB or Nambu) phase and the dynamical chiral symmetry preserved (DCS or Wigner) phase, meet at an interface. This interface effect, which is

measured by the interface tension and related quantities such as the interface entropy and the critical size of the bubble [81,82], has been investigated by lattice QCD simulation [83] and many effective model calculations [74,76–82,84–90]. On the other hand, it has been found for a long time that in the hadronization process there exists a so-called entropy puzzle; that is, the entropy density of the quark-gluon phase is always larger than that of the hadron phase in both the hadronization (DCS to DCSB) process and the deconfinement (DCS restoration) process [81,86,91–93], and thus the hadronization process seems to be impossible according to the increasing entropy principle. Effective model calculations have provided hints for that considering the interface entropy might solve this puzzle [81,86]. To make this solid, it is imperative to study the problem and solve the puzzle via a sophisticated continuum QCD approach.

It has been known that the Dyson-Schwinger equations (DSEs), a nonperturbative method of QCD [94–96], are successful in describing QCD phase transitions (e.g., Refs. [23–42,96,97]) and hadron properties (for reviews, see Ref. [96]). We then, in this paper, take the DSE method to calculate the uniform entropy density directly and include the interface entropy in the free-energy expression approximation with the particle number density determined by the DSE method being the input. We find that the interface entropy induced by the interface production is significant to solve the entropy puzzle. As the interface part is taken into account, the total entropy density of the two phases switches into the right order, which drives the quark-gluon phase into the hadron phase during the hadronization process. We also find that the interface entropy is proportional to the area, and this leads to a natural explanation to the area law of the entropy [98,99].

*yxliu@pku.edu.cn

The remainder of this paper is organized as follows. In Sec. II, we describe briefly the framework of DSEs of QCD at finite temperature T and finite chemical potential μ . In Sec. III, we display the results on the phase transitions and the thermodynamic properties. Then, we introduce the interface thermodynamics and depict the results in Sec. IV. Finally, Sec. V provides a summary and remark.

II. QUARK GAP EQUATION AND THERMODYNAMIC PROPERTY

In the framework of DSEs, the quark gap equation at finite temperature and quark chemical potential reads

$$S(\vec{p}, \tilde{\omega}_n)^{-1} = i\vec{\gamma} \cdot \vec{p} + i\gamma_4 \tilde{\omega}_n + m_0 + \Sigma(\vec{p}, \tilde{\omega}_n), \quad (1)$$

$$\begin{aligned} \Sigma(\vec{p}, \tilde{\omega}_n) &= T \sum_{l=-\infty}^{\infty} \int \frac{d^3 q}{(2\pi)^3} g^2 D_{\mu\nu}(\vec{p} - \vec{q}, \Omega_{nl}; T, \mu) \\ &\times \frac{\lambda^a}{2} \gamma_\mu S(\vec{q}, \tilde{\omega}_l) \frac{\lambda^a}{2} \Gamma_\nu(\vec{q}, \tilde{\omega}_l, \vec{p}, \tilde{\omega}_n), \end{aligned} \quad (2)$$

where m_0 is the current quark mass and $\tilde{\omega}_n = \omega_n + i\mu$ with $\omega_n = (2n+1)\pi T$ being the quark Matsubara frequency, μ the quark chemical potential, and $\Omega_{nl} = \omega_n - \omega_l$. $D_{\mu\nu}$ is the dressed-gluon propagator, and Γ_ν is the dressed quark-gluon interaction vertex.

The gap equation's solution can be decomposed as

$$\begin{aligned} S(\vec{p}, \tilde{\omega}_n)^{-1} &= i\vec{\gamma} \cdot \vec{p} A(\vec{p}^2, \tilde{\omega}_n^2) \\ &+ i\gamma_4 \tilde{\omega}_n C(\vec{p}^2, \tilde{\omega}_n^2) + B(\vec{p}^2, \tilde{\omega}_n^2). \end{aligned} \quad (3)$$

The dressed-gluon propagator has the form

$$g^2 D_{\mu\nu}(\vec{k}, \Omega_{nl}) = P_{\mu\nu}^T D_T(\vec{k}^2, \Omega_{nl}^2) + P_{\mu\nu}^L D_L(\vec{k}^2, \Omega_{nl}^2), \quad (4)$$

where $P_{\mu\nu}^{T,L}$ are, respectively, the transverse and longitudinal projection operators, and

$$D_T(k_\Omega) = \mathcal{D}(k_\Omega^2, 0), \quad D_L(k_\Omega) = \mathcal{D}(k_\Omega^2, m_g^2), \quad (5)$$

where m_g is the thermal mass of the gluon and can be taken as $m_g^2 = 16/5(T^2 + 6\mu^2/(5\pi^2))$ according to perturbative QCD calculations [100,101].

We employ the infrared constant model (Qin-Chang model) [102] for the dressed-gluon propagator that qualitatively reproduces the features of the results of modern DSE calculations and lattice QCD simulations [103–114], which reads

$$\begin{aligned} \mathcal{D}(k_\Omega^2, m_g^2) &= 8\pi^2 D \frac{1}{\omega^4} e^{-s_\Omega/\omega^2} \\ &+ \frac{8\pi^2 \gamma_m}{\ln[\tau + (1 + s_\Omega/\Lambda_{\text{QCD}}^2)^2]} \mathcal{F}(s_\Omega), \end{aligned} \quad (6)$$

with $\mathcal{F}(s_\Omega) = (1 - \exp(-s_\Omega/4m_t^2))/s_\Omega$, $s_\Omega = \Omega^2 + \vec{k}^2 + m_g^2$, $\tau = e^2 - 1$, $m_t = 0.5 \text{ GeV}$, $\gamma_m = 12/25$, and $\Lambda_{\text{QCD}} = 0.234 \text{ GeV}$.

To include the temperature screening effect which would screen the interaction when we calculate the thermodynamic properties of QCD, we remedy the coupling D to $D(T, \mu)$ in a similar way as in Refs. [31,33],

$$D(T, \mu) = \begin{cases} D, & T < T_p, \\ \frac{a}{b(\mu) + \ln[T'/\Lambda_{\text{QCD}}]}, & T \geq T_p, \end{cases} \quad (7)$$

where $T' = \sqrt{T^2 + 6\mu^2/(5\pi^2)}$ and T_p is the temperature at which the thermal screening effect emerges. At $\mu = 0$, we take $T_p = T_c(\mu = 0)$ with T_c the chiral phase transition temperature and $a = 0.029 \text{ GeV}^2$, $b = 0.432$, and while the phase transition temperature $T_c(\mu)$ would change as the chemical potential changes, herein we still apply $T_p = T_c(\mu)$ and adjust the value of b at every chemical potential to make the coupling strength $D(T_c(\mu), \mu) = D$.

For the quark-gluon interaction vertex, we take the approximation $\Gamma_\nu(\vec{q}, \tilde{\omega}_l, \vec{p}, \tilde{\omega}_n) = \gamma_\nu$, which has been widely implemented in Dyson-Schwinger equation calculations and shown to be quite a good approximation in studying hadron properties [115–126] and QCD phase transitions (for a comparison with the result in a sophisticated vertex, see, e.g., Ref. [42]).

The quark pressure is given by the tree-level auxiliary-field effective action [127] in stationary phase approximation,

$$P[S] = \frac{T}{V} \ln Z = \frac{T}{V} \left(\text{Tr} \ln [\beta S^{-1}] - \frac{1}{2} \text{Tr}[\Sigma S] \right), \quad (8)$$

where $\beta = 1/T$ and the self-energy $\Sigma = S^{-1} - S_0^{-1}$ with S_0 the free quark propagator. However, this definition holds ultraviolet divergence, which should be subtracted to get the physical pressure. Herein, we take the subtraction scheme according to the relation [128]

$$\begin{aligned} T \sum_{n=-\infty}^{\infty} f(p_0 = i\omega_n + \mu) &= \int_{-i\infty}^{i\infty} \frac{dp_0}{2\pi i} f(p_0) + \oint \frac{dp_0}{2\pi i} f(p_0) \\ &- \int_{-i\infty+\mu+\epsilon}^{i\infty+\mu+\epsilon} \frac{dp_0}{2\pi i} f(p_0) \frac{1}{e^{(p_0-\mu)/T} + 1} \\ &- \int_{-i\infty+\mu-\epsilon}^{i\infty+\mu-\epsilon} \frac{dp_0}{2\pi i} f(p_0) \frac{1}{e^{-(p_0-\mu)/T} + 1}, \end{aligned} \quad (9)$$

with the integral contour shown in Fig. 1. The second contour integration on rhs in Eq. (9) is a term independent of temperature. This term will get a finite value if there is singularity within the contour. For the Nambu solution of

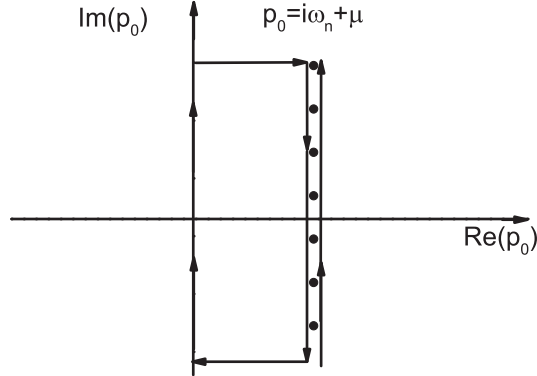


FIG. 1. Sketch of the integral contour in Eq. (9).

the gap equation, owing to the dynamical mass, there is no singularity within the contour,¹ and thus it contributes only in the Wigner phase. The last two terms represent the temperature effect, and it can be seen that the exponential damping factor ensures that there is no additional divergence when including the temperature effect. The first integration term on the rhs in Eq. (9) contains the divergence of the effective action, and hence the thermal properties could be obtained by subtracting this integration from the numerical data, the lhs. The practical algorithm to fulfill the subtraction is straightforward [41]: solve the quark gap equation at a given (μ, T) pair for a large number of Matsubara frequencies; at each (μ, T) , obtain smooth interpolations in p_0 for the three scalar functions in Eq. (3); and then compute the difference between the sum, lhs, and the first integration, rhs.

III. PHASE DIAGRAM AND UNIFORM THERMAL PROPERTIES

We first give the phase diagram in the μ - T plane of the two flavor system with renormalization-group-invariant current-quark mass $m_{u,d} = 6$ MeV via the chiral susceptibility criterion with the susceptibility being defined in the framework of DSEs as [30,42]

¹Herein, there exists in fact a problem that, because the propagator of the physical quark in the Nambu phase will always have a certain mass pole structure, the quark propagator of the Nambu phase may involve singularities within the contour. However, if we take the $M(\vec{p}^2 = 0, \omega_0)$ in Euclidean space as an approximation of the physical mass poles, we find that for the Nambu phase $M(\vec{p}^2 = 0, \omega_0, \mu)$ is always larger than the μ in the case beyond the chiral limit. This fact leads us then to this argument. Meanwhile, in our practical calculation, due to the fact we mentioned in the follows and the numerical data in Euclidean space manifest, only the first term of the formula enters in the regulation procedure. We neglect then the contribution of the singularities of the quark propagator of Nambu phase temporarily.

$$\chi_q = \frac{\partial B(\vec{p}^2 = 0, \tilde{\omega}_n^2)}{\partial m_0}. \quad (10)$$

In the calculation, the parameter(s) taken is (are), as in many previous works, $\omega = 0.5$ GeV with the restriction $D\omega = (0.8$ GeV)³.

It has been known that, in the first-order phase transition region, the susceptibility of the DCSB phase and that of the DCS phase diverge at different locations. The set of the states for the susceptibility of each phase to diverge identify a boundary. The region between the two boundaries is just the coexistence region which consists of a stable phase and a metastable phase (in detail, the DCSB phase changes from stable to metastable, and the DCS phase varies from metastable to stable, as the chemical potential increases at a certain temperature). In the crossover region, the susceptibility does not diverge, and thus, as usual, we define the location for the susceptibility to take its maximum as the phase transition point. Since the critical end point (CEP) connects the two regions and thus will combine both the characters, that is, the susceptibilities of the two phases diverge at the same location. The obtained phase diagram is shown in Fig. 2. It is evident that the crossover takes place in the low chemical potential region. Beyond the location of the CEP $(\mu_q^{\chi,E}, T^{\chi,E}) = (111, 128)$ MeV, the chiral phase transition of QCD becomes a first-order transition. Since the nucleation process describes the phase transition from a metastable phase to a stable phase, we find that the chiral phase transition takes place at different locations for different processes [81]. The DCSB to DCS phase transition takes place at higher chemical potential until the higher bound of the coexistence region, while for the opposite process, the hadronization process is accomplished at low chemical potential until the lower bound of the coexistence region.

The phase diagram could be converted into the plane of temperature and baryon number density n_B with the relation

$$n_B = \frac{1}{3} n_q = \frac{1}{3} \frac{\partial P}{\partial \mu_q}, \quad (11)$$

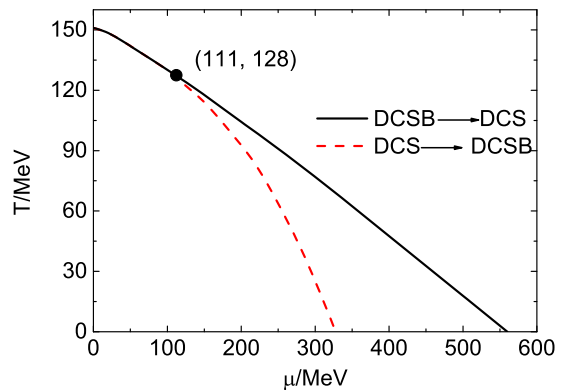


FIG. 2. Obtained phase diagram in terms of temperature and quark chemical potential.

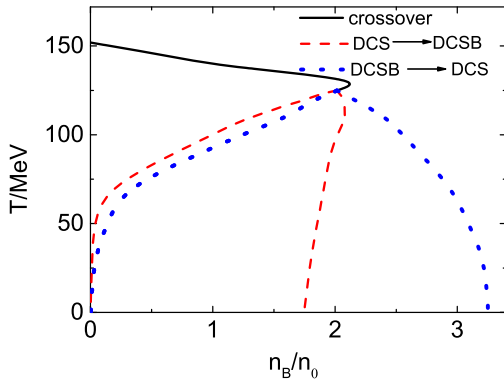


FIG. 3. Obtained phase diagram in terms of temperature and baryon number density.

where μ_q refers to the quark chemical potential and n_q is the quark number density.

The obtained result is displayed in Fig. 3. The number densities of the two phases in the hadronization process are shown as the dashed curve, while those for the opposite process are depicted as the dotted curve. For each curve, there are two values at every certain temperature corresponding to the different number densities of the two phases. The larger one is the number density of the DCS phase, and the smaller one is that of the DCSB phase. As the temperature increases, they converge gradually at the CEP and become identical as the phase transition becomes a crossover. The energy density at the CEP is $E_g = 0.377 \text{ GeV} \cdot \text{fm}^{-3}$, and the baryon number density at the CEP is $n_B = 2.02n_0$ with $n_0 = 0.16 \text{ fm}^{-3}$, the saturation baryon number density of nuclear matter.

After that, we obtain the entropy density with the Duhem-Gibbs relation:

$$s_V = \frac{1}{T}(\epsilon + P - \mu n) = \frac{\partial P}{\partial T}. \quad (12)$$

The obtained results are shown in Fig. 4. It is evident that, for the phase transition from the DCSB to the DCS phase, the entropy density increases; while in the opposite

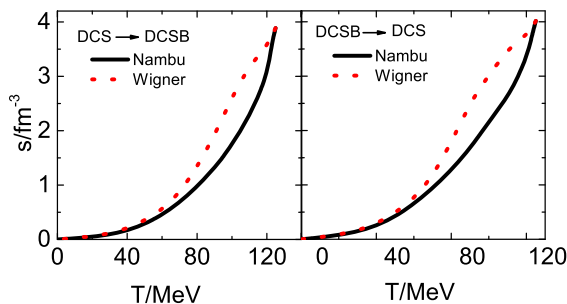


FIG. 4. Obtained variation behavior of the s_V of the two phases in the first-order phase transition region with respect to temperature. Left panel: in the process from the DCS to DCSB phase; right panel: in the process from the DCSB to DCS phase.

process, the hadronization process, the entropy density of the DCS phase is still larger than that of the DCSB phase. It is apparent that this result violates the increasing entropy principle and hence makes it impossible for the phase transition from DCS to DCSB (hadronization) to take place automatically as temperature decreases, which is just the so-called entropy puzzle in the hadronization process. People might assume that after the hadronization process the released energy will increase the volume of system and, in turn, the total entropy still increases even though the entropy density of the system decreases. However, during the phase transition process, when the hadron bubble emerges in the DCS state, the interface tension constrains the increase of the bubble's volume. Thus, at this moment, the key to solving the entropy puzzle would be the inhomogeneity, i.e., the interface between the distinct phases of the system [81]. When the phase transition takes place, the two phases meet at an interface, which gives additional interface entropy. With this part retrieved for the total entropy, we may find that the total entropy density increases in the hadronization process.

IV. THERMODYNAMICS INCLUDING THE INTERFACE EFFECT

As mentioned above, with the Duhem-Gibbs relation, we can only get the thermodynamic properties of uniform bulk matters. Reference [81] provides a hint that, to solve the entropy puzzle, it is necessary to consider the effect of the interface. As the contribution of the interface is taken into account, the total free-energy variance of the matter around the interface holds,

$$dF = -\Delta P dV - S_A dT + \gamma dA, \quad (13)$$

where ΔP is the pressure difference between the two phases, S_A is the interface entropy, γ is the interface tension, and A is the interface area. For a stable interface, with the Maxwell relation, we obtain straightforwardly the relation between the interface entropy S_A and interface tension as

$$S_A = A \cdot s_A = A \left(\frac{\partial S_A}{\partial A} \right)_{V,T} = -A \left(\frac{\partial \gamma}{\partial T} \right)_{V,T}, \quad (14)$$

where s_A is the interface entropy density.

The total entropy density of the system could then be written as

$$s_{\text{tot}}(T) = s_V + \frac{A}{V} s_A, \quad (15)$$

where V and A are, respectively, the volume of the system and the area of the interface. The ratio A/V is hard to obtain completely and accurately. However, we can intuitively make an assumption that the system is composed of lattices

with length $2R$, and each of the lattices includes a spherical bubble with radius R . Then, the relation between the A and the V can be approximately given as $A/V \approx \pi/(2R)$, where the R is the average radius of the bubbles formed during the phase transition process. Such a radius can be extracted from the stationary condition of free energy [combining the geometric property and the result from Eq. (13)] as

$$\frac{3}{\pi}R = \frac{dV}{dA} = \frac{\gamma}{\Delta P}. \quad (16)$$

Taking the phenomenological expansion of the free-energy density for the first-order phase transition system [82], we have

$$f(\vec{r}) = n\mu + \frac{1}{2}C(\nabla n)^2, \quad (17)$$

where $C = \frac{a^2}{n_B^2}E_g$. To evaluate the free energy of our interested system in the DSE calculation, we take n_B and E_g to be the baryon number density and the energy density at the CEP. For the parameter a , the measure of the interface's thickness, we choose it to be 0.33 fm as that in Refs. [81,87].

The density distribution could be obtained through the variation of free energy under the restriction of normalization according to the equilibration condition,

$$0 = \delta \int \left\{ n(\vec{r})\mu_T[n] + \frac{1}{2}C(\nabla n)^2 - \mu_0 n(\vec{r}) \right\} d\vec{r}, \quad (18)$$

where $\mu_T[n]$ and μ_0 are the distribution of chemical potential and uniform chemical potential, respectively.

The equation of motion for the spherical case could be written as

$$\Delta f_T + \frac{1}{2}C\left(\frac{\partial n}{\partial r}\right)^2 = 0, \quad (19)$$

where $\Delta f_T = f_T(n) - f_M(n)$ is the difference between the free-energy densities of the uniform matter at different conditions defined in Ref. [82] and f_M is the Maxwell construction of the free energy defined as

$$f_M(n) = f_T(n_L) + \frac{f_T(n_H) - f_T(n_L)}{n_H - n_L}(n - n_L), \quad (20)$$

where n_H and n_L are the densities of the two coexisting phases. Δf_T vanishes at the boundary and is positive in between and thus can be considered as the free energy gained by undergoing a phase mixture. The interface tension which is the deficit in free energy per unit interface area could then be expressed as

$$\gamma(T) = \int_{-\infty}^{\infty} \Delta f_T dx = \int_{n_L}^{n_H} \sqrt{\frac{C}{2} \Delta f_T(n)} dn. \quad (21)$$

The equation of motion has been used to obtain the second relation in Eq. (21). This relation is significant since it indicates that the interface tension is independent of the size scale of the system and thus an intensive quantity. With the relation in Eq. (14), we find that the interface entropy is proportional to the area of the interface. Generally, entropy is an extensive quantity with $S \sim R^3$, but the interface entropy satisfies $S_A \sim R^2$. Especially in the strong coupling limit, the uniform entropy of strongly interacting particles is small, and thus the interface part takes up a great proportion. The total entropy of the system will then tend to satisfy the area law in the limit. Therefore, the area law for the entropy indicates that the system becomes strongly coupled, and the interface effect decides most of the thermal properties of the system. Our present result provides evidence for the area law of the entropy [98,99] directly from the view of strong-interaction theory (QCD).

After solving the equation of motion, we get directly the density distribution at every temperature from the DSE approach. The obtained results of the baryon number density distribution are exhibited in Fig. 5. It is apparent that, for the process from the DCS phase to the DCSB phase, the hadronization process, the DCSB phase grows up inside the bubble as the radius gets larger, and the DCS phase plays

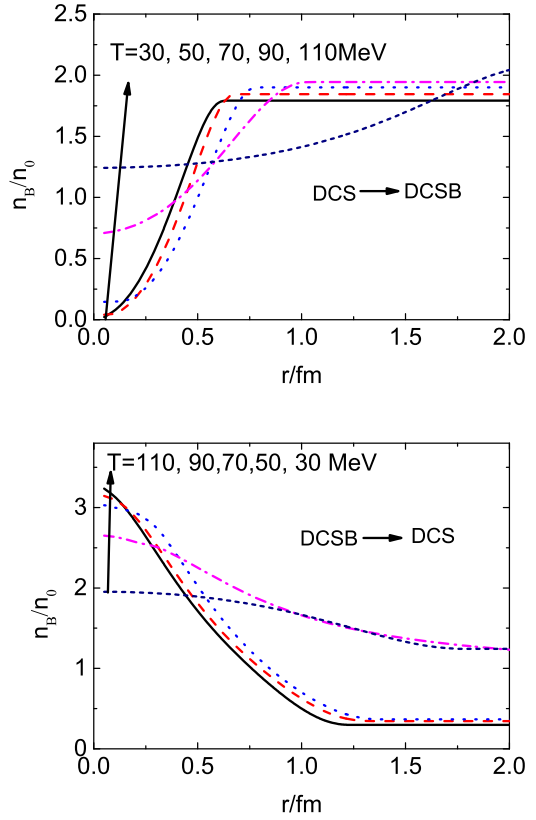


FIG. 5. Obtained baryon number density distribution at some temperature T in the two processes. Upper panel: for the process from the DCS to DCSB phase; lower panel: for the process from the DCSB to DCS phase.

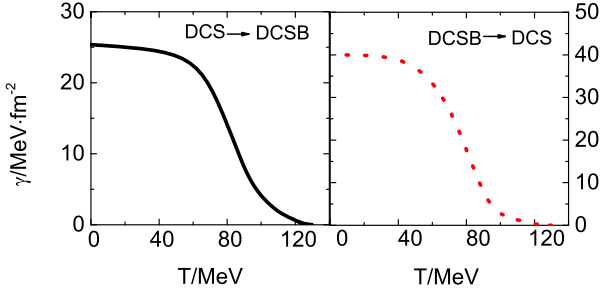


FIG. 6. Obtained variation behavior of the interface tension with respect to temperature. Left panel: for the process from the DCS to DCSB phase; right panel: for the process from the DCSB to DCS phase.

the role of the surrounding. While for the process from DCSB to DCS phase, the feature is just in the opposite.

The interface tension could be obtained straightforwardly through Eq. (21). In Fig. 6, we show our results of the temperature dependence of the interface tension for the two processes. It is evident that the interface tension of the hadronization process is smaller than that of the opposite at a certain temperature, due to the fact that the particle density distribution regions are different. The interface tension at zero temperature is 25.4 MeV/fm² for the hadronization process and 40.0 MeV/fm² for the opposite. Such results coincide with those given in other calculations (e.g., Refs. [76,81,82]) excellently. As the temperature increases, the interface tension decreases monotonically and vanishes near the CEP. For the convenience of being able to implement it elsewhere, we give approximately the temperature dependence of the interface tension in the form

$$\gamma(T) = a + b e^{(c/T+d/T^2)}, \quad (22)$$

with parameters listed in Table I.

We take then the first-order derivative of the interface tension with respect to temperature and obtain the interface entropy density. The obtained results of the temperature dependence of the interface entropy density in the two phase transition processes are shown in Fig. 7. Our above discussion manifests that the interface tension and the interface entropy make a contribution in the coexistence region, owing to the difference of the particle number densities of the two phases; thus, it vanishes at the CEP. Figure 7 shows obviously that, in both processes, the interface entropy densities experience a rapid increase at intermediate temperature and tend to be zero at zero temperature and at the CEP, as expected in general.

TABLE I. Fitted parameters of interface tension in Eq. (22).

	a /(MeV/fm ²)	b /(MeV/fm ²)	c / MeV	d /GeV ²
DCS → DCSB	25.4	-1.5	736	-0.048
DCSB → DCS	40.0	-8.1	399	-0.025

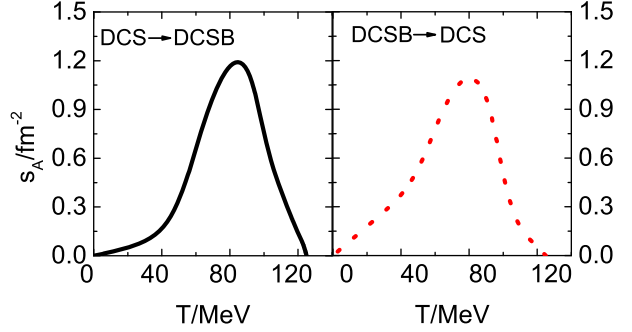


FIG. 7. Obtained temperature dependence of the interface entropy density in the two processes. Left panel: for the process from the DCS to DCSB phase; right panel: for the process from the DCSB to DCS phase.

After that, we identify the bubble size to obtain the total entropy density. The typical bubble size during the phase transition could be estimated through Eq. (16). We illustrate the obtained results as the solid lines in Fig. 8. It is apparent that the radius barely changes at low temperature, until about $T \sim 110$ MeV, and the radius increases drastically thereafter in both the processes. In more detail, the radius in hadronization (from DCS to DCSB) process is smaller at the same temperature since the process takes place at lower chemical potential (density).

Combining the results obtained above, we can get eventually the contribution of the interface entropy to the total entropy density ($\frac{A}{V} s_A = \frac{\pi}{2R} s_A$) of the system. In Sec. III, we have the entropy density of the bulk matter without the interface, which shows that, in both the processes, the entropy density of the DCS phase is larger than that of the DCSB phase, which violates the increasing entropy principle during the hadronization process. After adding the contribution of the interface entropy density to the total entropy density, we find that the total entropy density of the system increases in both the phase transition processes as shown in Fig. 9.

Recalling Eq. (16) and the derivation process, one can notice that we have not yet considered the thickness of the

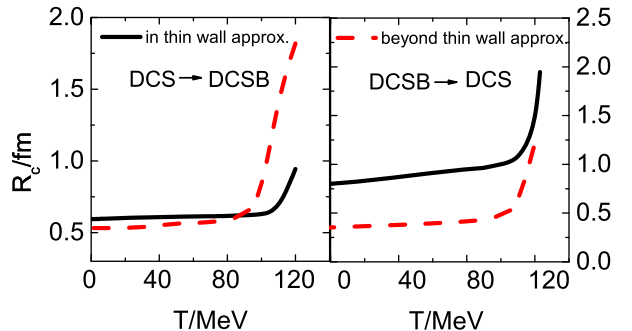


FIG. 8. Obtained temperature dependence of the bubble size in the two process. Left panel: in the process from the DCS to DCSB phase; right panel: in the process from the DCSB to DCS phase.

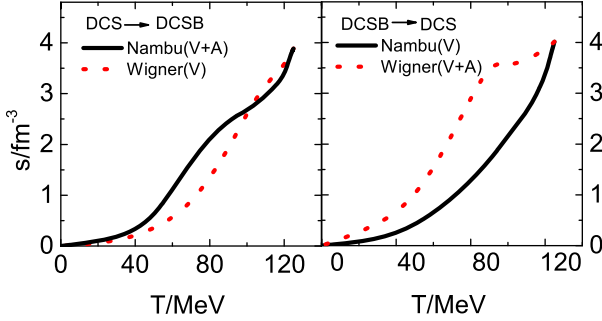


FIG. 9. Obtained temperature dependence of the total entropy density of the system with the bubble size determined by Eq. (16). Left panel: for the process from the DCS to DCSB phase; right panel: for the process from the DCSB to DCS phase.

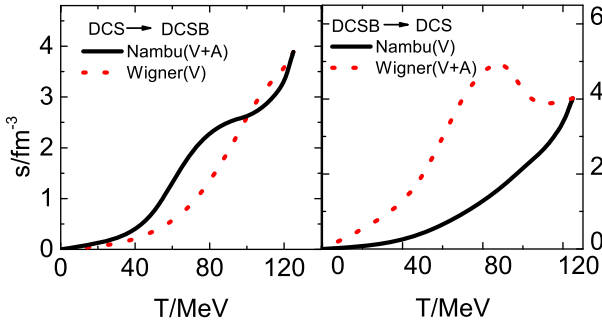


FIG. 10. Obtained temperature dependence of the total entropy density with the bubble size determined beyond the thin-wall approximation. Left panel: for the process from the DCS to DCSB phase; right panel: for the process from the DCSB to DCS phase.

bubble's surface except for introducing a parameter in the free-energy expansion to determine the interface tension. The above mentioned method is usually denoted as the thin-wall approximation. In fact, one can determine the bubble size directly from the density distribution, that is, namely, that beyond the thin-wall approximation, where the size reads as the radius corresponding to the steepest change of the density distribution (the results at some temperatures have been displayed in Fig. 5). With such a definition of the bubble size, we can also get the radius of the bubble (shown as the dashed line in Fig. 8) and the interface entropy density. In turn, we obtain the temperature dependence of the total entropy density as illustrated in

Fig. 10. It manifests evidently that, when altering the definition of the size, the total entropy density in each of the two phase transition processes changes quantitatively, but not qualitatively. In both cases, the interface effect modifies the total entropy density of the system and makes the hadronization process coincide with the increasing entropy principle.

V. SUMMARY

In summary, we studied some thermodynamic properties of QCD matter, especially those in the first-order phase transition region via the Dyson-Schwinger equations approach. We obtained the phase diagram of the chiral phase transition in terms of the temperature and the chemical potential and that in terms of temperature and baryon number density with a proper subtraction scheme to get the quarks' pressure and the related thermal quantities of the system. We calculated the entropy densities of both the DCSB and the DCS phases in the first-order phase transition region and found that the entropy density of the DCS phase is always larger than that of the DCSB phase in both the phase transition processes of uniform bulk matter. We then took the free-energy expansion scheme with the particle number density distribution obtained in the DSE calculation being the input and included the contribution of the interface demonstrating the inhomogeneity of the coexistence region. We calculated further the interface tension and the interface entropy density and found an area law for the interface entropy. After taking the interface effect into account, we observed that the total entropy density increases in both the DSCB to DCS and the DCS to DCSB processes of the first-order phase transition and thus solved the entropy puzzle in the hadronization process. In addition, we would like to mention that our present work provides evidence for the violation of the increasing entropy principle in some processes possibly resulting from having not taken all the effects, for instance, the structure and the entanglement among the ingredients, completely.

ACKNOWLEDGMENTS

The work was supported by the National Natural Science Foundation of China under Contract No. 11435001 and the National Key Basic Research Program of China under Contracts No. G2013CB834400 and No. 2015CB856900.

-
- [1] R. D. Pisarski and F. Wilczek, *Phys. Rev. D* **29**, 338 (1984).
[2] K. Rajagopal, *Nucl. Phys.* **A661**, 150 (1999).

- [3] D. N. S. A. Committee *et al.*, arXiv:0809.3137.
[4] P. Braun-Munzinger and J. Wambach, *Rev. Mod. Phys.* **81**, 1031 (2009).

- [5] K. Fukushima and T. Hatsuda, *Rept. Prog. Phys.* **74**, 014001 (2011).
- [6] O. Philipsen, *Prog. Part. Nucl. Phys.* **70**, 55 (2013).
- [7] Y. Hatta and T. Ikeda, *Phys. Rev. D* **67**, 014028 (2003).
- [8] M. Buballa, *Phys. Rep.* **407**, 205 (2005).
- [9] C. Ratti, M. A. Thaler, and W. Weise, *Phys. Rev. D* **73**, 014019 (2006).
- [10] B. J. Schaefer, J. M. Pawlowski, and J. Wambach, *Phys. Rev. D* **76**, 074023 (2007).
- [11] W. J. Fu, Z. Zhang, and Y. X. Liu, *Phys. Rev. D* **77**, 014006 (2008).
- [12] C. Sasaki, B. Friman, and K. Redlich, *Phys. Rev. D* **77**, 034024 (2008).
- [13] M. Ciminale, R. Gatto, N. D. Ippolito, G. Nardulli, and M. Ruggieri, *Phys. Rev. D* **77**, 054023 (2008).
- [14] P. Costa, M. C. Ruivo, and C. A. de Sousa, *Phys. Rev. D* **77**, 096001 (2008).
- [15] K. Fukushima, *Phys. Rev. D* **77**, 114028 (2008).
- [16] H. Abuki, R. Anglani, R. Gatto, G. Nardulli, and M. Ruggieri, *Phys. Rev. D* **78**, 034034 (2008).
- [17] Y. Zhao, L. Chang, W. Yuan, and Y.-x. Liu, *Eur. Phys. J. C* **56**, 483 (2008).
- [18] B. J. Schaefer and M. Wagner, *Phys. Rev. D* **79**, 014018 (2009).
- [19] H. Mao, J. S. Jin, and M. Huang, *J. Phys. G* **37**, 035001 (2010).
- [20] A. Ayala, A. Bashir, C. A. Dominguez, E. Gutiérrez, M. Loewe, and A. Raya, *Phys. Rev. D* **84**, 056004 (2011).
- [21] T. Sasaki, Y. Sakai, H. Kouno, and M. Yahiro, *Phys. Rev. D* **82**, 116004 (2010); L. J. Jiang, X. Y. Xin, K. L. Wang, S. X. Qin, and Y. X. Liu, *Phys. Rev. D* **88**, 016008 (2013).
- [22] X. Y. Xin, S. X. Qin, and Y. X. Liu, *Phys. Rev. D* **89**, 094012 (2014).
- [23] A. Bender, D. Blaschke, Y. Kalinovsky, and C. D. Roberts, *Phys. Rev. Lett.* **77**, 3724 (1996).
- [24] A. Bender, G. I. Poulis, C. D. Roberts, S. M. Schmidt, and A. W. Thomas, *Phys. Lett. B* **431**, 263 (1998).
- [25] D. Blaschke, C. D. Roberts, and S. Schmidt, *Phys. Lett. B* **425**, 232 (1998).
- [26] P. Maris, A. Raya, C. D. Roberts, and S. M. Schmidt, *Eur. Phys. J. A* **18**, 231 (2003).
- [27] H. Chen, W. Yuan, L. Chang, Y. X. Liu, T. Klahn, and C. D. Roberts, *Phys. Rev. D* **78**, 116015 (2008).
- [28] C. S. Fischer, *Phys. Rev. Lett.* **103**, 052003 (2009); C. S. Fischer and J. A. Mueller, *Phys. Rev. D* **80**, 074029 (2009).
- [29] J. A. Mueller, C. S. Fischer, and D. Nickel, *Eur. Phys. J. C* **70**, 1037 (2010).
- [30] S. X. Qin, L. Chang, H. Chen, Y. X. Liu, and C. D. Roberts, *Phys. Rev. Lett.* **106**, 172301 (2011).
- [31] S. X. Qin, L. Chang, Y. X. Liu, and C. D. Roberts, *Phys. Rev. D* **84**, 014017 (2011).
- [32] S. X. Qin and D. H. Rischke, *Phys. Rev. D* **88**, 056007 (2013).
- [33] F. Gao, S. X. Qin, Y. X. Liu, C. D. Roberts, and S. M. Schmidt, *Phys. Rev. D* **89**, 076009 (2014).
- [34] X. Y. Xin, S. X. Qin, and Y. X. Liu, *Phys. Rev. D* **90**, 076006 (2014).
- [35] M. He, Y. Jiang, W. M. Sun, and H. S. Zong, *Phys. Rev. D* **77**, 076008 (2008); M. He, F. Hu, W. M. Sun, and H. S. Zong, *Phys. Lett. B* **675**, 32 (2009); B. Wang, Z. F. Cui, W. M. Sun, and H. S. Zong, *Few-Body Syst.* **55**, 47 (2014); C. Shi, Y. L. Wang, Y. Jiang, Z. F. Cui, and H. S. Zong, *J. High Energy Phys.* **07** (2014) 014.
- [36] S. S. Xu, Z. F. Cui, B. Wang, Y. M. Shi, Y. C. Yang, and H. S. Zong, *Phys. Rev. D* **91**, 056003 (2015); Y. Lu, Z. F. Cui, Z. Pan, C. H. Chang, and H. S. Zong, *Phys. Rev. D* **93**, 074037 (2016).
- [37] C. S. Fischer, J. Luecker, and J. A. Mueller, *Phys. Lett. B* **702**, 438 (2011); C. S. Fischer and J. Luecker, *Phys. Lett. B* **718**, 1036 (2013); C. S. Fischer, J. Luecker, and C. A. Welzbacher, *Phys. Rev. D* **90**, 034022 (2014).
- [38] *Nucl. Phys.* **A931**, 774 (2014).
- [39] E. Gutiérrez, A. Ahmad, A. Ayala, A. Bashir, and A. Raya, *J. Phys. G* **41**, 075002 (2014).
- [40] G. Eichmann, C. S. Fischer, and C. A. Welzbacher, *Phys. Rev. D* **93**, 034013 (2016).
- [41] F. Gao, J. Chen, Y. X. Liu, S. X. Qin, C. D. Roberts, and S. M. Schmidt, *Phys. Rev. D* **93**, 094019 (2016).
- [42] F. Gao and Y. X. Liu, *Phys. Rev. D* **94**, 076009 (2016).
- [43] J. M. Pawlowski, *Ann. Phys. (Amsterdam)* **322**, 2831 (2007).
- [44] L. Fister and J. M. Pawlowski, *Phys. Rev. D* **88**, 045010 (2013).
- [45] M. Mitter, J. M. Pawlowski, and N. Strodthoff, *Phys. Rev. D* **91**, 054035 (2015).
- [46] N. Mueller and J. M. Pawlowski, *Phys. Rev. D* **91**, 116010 (2015).
- [47] N. Christiansen, M. Haas, J. M. Pawlowski, and N. Strodthoff, *Phys. Rev. Lett.* **115**, 112002 (2015).
- [48] W. J. Fu and J. M. Pawlowski, *Phys. Rev. D* **92**, 116006 (2015); **93**, 091501(R) (2016).
- [49] G. Boyd, J. Engels, F. Karsch, E. Laermann, C. Legeland, M. Lutgemeier, and B. Petersson, *Nucl. Phys.* **B469**, 419 (1996).
- [50] F. Karsch, *Lect. Notes Phys.* **585**, 209 (2002).
- [51] Ph. de Forcrand and O. Philipsen, *Nucl. Phys.* **B642**, 290 (2002); **B673**, 170 (2003); Ph. de Forcrand and S. Kratochvila, *Nucl. Phys. B, Proc. Suppl.* **153**, 62 (2006).
- [52] Z. Fodor and S. D. Katz, *arXiv:0908.3341*; *Phys. Lett. B* **534**, 87 (2002); *J. High Energy Phys.* **03** (2002) 014; **04** (2004) 050.
- [53] M. D'Elia and M. P. Lombardo, *Phys. Rev. D* **67**, 014505 (2003).
- [54] C. Bernard, T. Burch, C. DeTar, J. Osborn, S. Gottlieb, E. B. Gregory, D. Toussaint, U. M. Heller, and R. Sugar, *Phys. Rev. D* **71**, 034504 (2005).
- [55] Y. Aoki, G. Endrodi, Z. Fodor, S. D. Katz, and K. K. Szabo, *Nature (London)* **443**, 675 (2006).
- [56] Y. Aoki, Z. Fodor, S. D. Katz, and K. K. Szabo, *Phys. Lett. B* **643**, 46 (2006).
- [57] C. R. Allton, M. Doring, S. Ejiri, S. J. Hands, O. Kaczmarek, F. Karsch, E. Laermann, and K. Redlich, *Phys. Rev. D* **71**, 054508 (2005).
- [58] R. V. Gavai and S. Gupta, *Phys. Rev. D* **71**, 114014 (2005); **78**, 114503 (2008).
- [59] Ph. de Forcrand and O. Philipsen, *Phys. Rev. Lett.* **105**, 152001 (2010); Ph. de Forcrand, J. Langelage, O. Philipsen, and W. Unger, *Phys. Rev. Lett.* **113**, 152002 (2014).
- [60] G. Endrodi, Z. Fodor, S. D. Katz, and K. K. Szabo, *J. High Energy Phys.* **04** (2011) 001.

- [61] O. Kaczmarek, F. Karsch, E. Laermann, C. Miao, S. Mukherjee, P. Petreczky, C. Schmidt, W. Soeldner, and W. Unger, *Phys. Rev. D* **83**, 014504 (2011).
- [62] A. Li, A. Alexandru, and K. F. Liu, *Phys. Rev. D* **84**, 071503 (2011).
- [63] F. Karsch, B. J. Schaefer, M. Wagner, and J. Wambach, *Phys. Lett. B* **698**, 256 (2011).
- [64] T. Bhattacharya *et al.*, *Phys. Rev. Lett.* **113**, 082001 (2014).
- [65] A. Bazavov *et al.*, *Phys. Rev. D* **85**, 054503 (2012); *Phys. Rev.* **86**, 034509 (2012).
- [66] P. Cea, L. Cosmai, and A. Papa, *Phys. Rev. D* **89**, 074512 (2014).
- [67] S. Gupta, N. Karthik, and P. Majumdar, *Phys. Rev. D* **90**, 034001 (2014).
- [68] M. Cheng *et al.* (HotQCD Collaboration), *Phys. Rev. D* **79**, 074505 (2009).
- [69] R. V. Gavai and S. Gupta, *Phys. Lett. B* **696**, 459 (2011).
- [70] A. Bazavov *et al.* (HotQCD Collaboration), *Phys. Rev. Lett.* **109**, 192302 (2012).
- [71] S. Borsanyi, Z. Fodor, S. D. Katz, S. Krieg, C. Ratti, and K. K. Szabó, *J. High Energy Phys.* **01** (2012) 138.
- [72] S. Borsanyi, Z. Fodor, S. D. Katz, S. Krieg, C. Ratti, and K. K. Szabo, *Phys. Rev. Lett.* **111**, 062005 (2013).
- [73] S. Borsanyi, Z. Fodor, S. D. Katz, S. Krieg, C. Ratti, and K. K. Szabo, *Phys. Rev. Lett.* **113**, 052301 (2014).
- [74] L. F. Palhares and E. S. Fraga, *Phys. Rev. D* **82**, 125018 (2010).
- [75] A. Holl, P. Maris, and C. D. Roberts, *Phys. Rev. C* **59**, 1751 (1999).
- [76] H. Heiselberg, C. J. Pethick, and E. F. Stoab, *Phys. Rev. Lett.* **70**, 1355 (1993).
- [77] L. F. Palhares and E. S. Fraga, *Proc. Sci. FACESQCD* (2010) 014.
- [78] D. Kroff and E. S. Fraga, *Phys. Rev. D* **91**, 025017 (2015).
- [79] S. M. de Carvalho, R. Negreiros, M. Orsaria, G. A. Contrera, F. Weber, and W. Spinella, *Phys. Rev. C* **92**, 035810 (2015).
- [80] I. F. Ranea-Sandoval, S. Han, M. G. Orsaria, G. A. Contrera, F. Weber, and M. G. Alford, *Phys. Rev. C* **93**, 045812 (2016).
- [81] W. Y. Ke and Y. X. Liu, *Phys. Rev. D* **89**, 074041 (2014).
- [82] J. Randrup, *Phys. Rev. C* **79**, 054911 (2009).
- [83] P. de Forcrand, B. Lucini, and M. Vettorazzo, *Nucl. Phys. Proc. Suppl.* **140**, 647 (2005).
- [84] M. B. Pinto, V. Koch, and J. Randrup, *Phys. Rev. C* **86**, 025203 (2012).
- [85] B. W. Mintz, R. Stiele, R. O. Ramos, and J. Schaffner-Bielich, *Phys. Rev. D* **87**, 036004 (2013).
- [86] J. Song, Z. T. Liang, Y. X. Liu, F. L. Shao, and Q. Wang, *Phys. Rev. C* **81**, 057901 (2010).
- [87] X. J. Wen, J. Y. Li, J. Q. Liang, and G. X. Peng, *Phys. Rev. C* **82**, 025809 (2010).
- [88] G. Lugones, A. G. Grunfeld, and M. A. Ajmi, *Phys. Rev. C* **88**, 045803 (2013).
- [89] A. F. Garcia and M. B. Pinto, *Phys. Rev. C* **88**, 025207 (2013).
- [90] C. J. Xia, G. X. Peng, E. G. Zhao, and S. G. Zhou, *Phys. Rev. D* **93**, 085025 (2016).
- [91] J.-P. Blaizot, E. Iancu, and A. Rebhan, *Phys. Rev. Lett.* **83**, 2906 (1999); *Phys. Rev. D* **63**, 065003 (2001).
- [92] V. Greco, C. M. Ko, and P. Levai, *Phys. Rev. C* **68**, 034904 (2003).
- [93] K. Yamazaki, T. Matsui, and G. Baym, *Nucl. Phys.* **A933**, 245 (2015).
- [94] C. D. Roberts and A. G. Williams, *Prog. Part. Nucl. Phys.* **33**, 477 (1994); C. D. Roberts and S. Schmidt, *Prog. Part. Nucl. Phys.* **45**, S1 (2000).
- [95] R. Alkofer and L. von Smekal, *Phys. Rep.* **353**, 281 (2001).
- [96] P. Maris and C. D. Roberts, *Int. J. Mod. Phys. E* **12**, 297 (2003); A. Bashir, L. Chang, I. C. Cloet, B. El-Bennich, Y. X. Liu, C. D. Roberts, and P. C. Tandy, *Commun. Theor. Phys.* **58**, 79 (2012); I. C. Cloet and C. D. Roberts, *Prog. Part. Nucl. Phys.* **77**, 1 (2014).
- [97] K. L. Wang, S. X. Qin, Y. X. Liu, L. Chang, C. D. Roberts, and S. M. Schmidt, *Phys. Rev. D* **86**, 114001 (2012).
- [98] M. Srednicki, *Phys. Rev. Lett.* **71**, 666 (1993).
- [99] J. Eisert, M. Cramer, and M. B. Plenio, *Rev. Mod. Phys.* **82**, 277 (2010).
- [100] N. Haque, M. G. Mustafa, and M. Strickland, *Phys. Rev. D* **87**, 105007 (2013).
- [101] M. H. Thoma, *Nucl. Phys.* **A638**, 317C (1998).
- [102] S. X. Qin, L. Chang, Y. X. Liu, C. D. Roberts, and D. J. Wilson, *Phys. Rev. C* **84**, 042202(R) (2011).
- [103] P. O. Bowman, U. M. Heller, D. B. Leinweber, M. B. Parappilly, and A. G. Williams, *Phys. Rev. D* **70**, 034509 (2004); P. O. Bowman, U. M. Heller, D. B. Leinweber, M. B. Parappilly, A. G. Williams, and J. B. Zhang, *Phys. Rev. D* **71**, 054507 (2005).
- [104] I. Bogolubsky, E. Ilgenfritz, M. Muller-Preussker, and A. Sternbeck, *Phys. Lett. B* **676**, 69 (2009).
- [105] P. Boucaud, M. E. Gomez, J. P. Leroy, A. Le Yaouanc, J. Micheli, O. Pene, and J. Rodriguez-Quintero, *Phys. Rev. D* **82**, 054007 (2010).
- [106] O. Oliveira and P. Bicudo, *J. Phys. G* **38**, 045003 (2011).
- [107] A. Cucchieri, D. Dudal, T. Mendes, and N. Vandersickel, *Phys. Rev. D* **85**, 094513 (2012).
- [108] A. C. Aguilar, D. Binosi, and J. Papavassiliou, *Phys. Rev. D* **86**, 014032 (2012).
- [109] A. Ayala, A. Bashir, D. Binosi, M. Cristoforetti, and J. Rodriguez-Quintero, *Phys. Rev. D* **86**, 074512 (2012).
- [110] D. Dudal, O. Oliveira, and J. Rodriguez-Quintero, *Phys. Rev. D* **86**, 105005 (2012).
- [111] S. Strauss, C. S. Fischer, and C. Kellermann, *Phys. Rev. Lett.* **109**, 252001 (2012).
- [112] A. Weber, *J. Phys. Conf. Ser.* **378**, 012042 (2012).
- [113] D. Zwanziger, *Phys. Rev. D* **87**, 085039 (2013).
- [114] B. Blossier, P. Boucaud, M. Brinet, F. De Soto, V. Morenas, O. Pene, K. Petrov, and J. Rodriguez-Quintero, *Phys. Rev. D* **87**, 074033 (2013).
- [115] H. J. Munczek, *Phys. Rev. D* **52**, 4736 (1995).
- [116] A. Bender, C. D. Roberts, and L. von Smekal, *Phys. Lett. B* **380**, 7 (1996).
- [117] C. J. Burden, L. Qian, C. D. Roberts, P. C. Tandy, and M. J. Thomson, *Phys. Rev. C* **55**, 2649 (1997).
- [118] P. Watson, W. Cassing, and P. C. Tandy, *Few-Body Syst.* **35**, 129 (2004).

- [119] P. Maris, *AIP Conf. Proc.* **892**, 65 (2007).
- [120] I. C. Cloët, A. Krassnigg, and C. D. Roberts, in *Proceedings of 11th International Conference on Meson-Nucleon Physics and the Structure of the Nucleon (MENU 2007), Juelich, Germany, 2007*, edited by H. Machner and S. Krewald (SLAC, Stanford, 2007), paper 125.
- [121] C. S. Fischer and R. Williams, *Phys. Rev. Lett.* **103**, 122001 (2009).
- [122] A. Krassnigg, *Phys. Rev. D* **80**, 114010 (2009).
- [123] A. Krassnigg and M. Blank, *Phys. Rev. D* **83**, 096006 (2011).
- [124] M. Blank and A. Krassnigg, *Phys. Rev. D* **84**, 096014 (2011); T. Hilger, C. Popovici, M. Gomez-Rocha, and A. Krassnigg, *Phys. Rev. D* **91**, 034013 (2015).
- [125] T. Hilger, M. Gomez-Rocha, and A. Krassnigg, *Phys. Rev. D* **91**, 114004 (2015).
- [126] M. Gomez-Rocha, T. Hilger, and A. Krassnigg, *Few-Body Syst.* **56**, 475 (2015); *Phys. Rev. D* **92**, 054030 (2015); **93**, 074010 (2016).
- [127] R. W. Haymaker, *Riv. Nuovo Cimento* **14**, 1 (1991).
- [128] J. I. Kapusta, *Finite-Temperature Field Theory* (Cambridge University Press, Cambridge, England, 1993).